J. Membrane Biol. 180, 137–145 (2001)
DOI: 10.1007/s002320010065

The Journal of
Membrane
Biology



# $ED_{50}$ *AP* Block Predictions for Phenyl Substituted and Unsubstituted *n*-Alkanols

**R. Hahin, A. Kondratiev***
Department of Biological Sciences, Northern Illinois University, Dekalb, IL 60115, USA

Received: 11 August 2000/Revised: 21 December 2000

**Abstract.** A series of *n*-alkanols and phenyl-substituted *n*-alkanols (Φ-alkanols) of increasing chain length and phenol were characterized for their ability to block action potentials (*AP*s) in frog sciatic nerves. *AP*s were recorded using the single sucrose-gap method. The degree of *AP* attenuation when the nerve was exposed to different concentrations of an alcohol was used to construct dose-response curves. The reciprocals of the half-blocking doses ($ED_{50}$s) were used to obtain a measure of the potency of the alcohols. For *n*-alkanols and Φ-alkanols, increasing the chain length by the addition of a methylene group increased the potency on average by 3.1 for both groups of alkanols. The addition of a phenyl group caused a potency increase that ranged between the values of 77 and 122. The $ED_{50}$ for both groups of alkanols could not be solely predicted by the log octanol-water partition coefficient ($K_{OW}$). Using linear solvation energy relations (*LSER*), the log $ED_{50}$ could be described as a linear combination of the intrinsic (van der Waals) molar volume ($V_I$), polarity ($P$), and hydrogen bond acceptor basicity (β) and donor acidity (α). Size alone could not predict the $ED_{50}$ for both *n*-alkanols and Φ-alkanols. The results are consistent with the hypothesis that alkanols bind to and interact with Na channels to cause *AP* block. Phenyl group addition to an alkanol markedly increases the molecule's potency.

**Key words:** Action potential block — Anesthesia — Alkanols — Phenyl substitution

## Introduction

The molecular basis of anesthesia is incompletely understood. Alkanols have been used as model anesthetic molecules. Early work suggested that alkanols act to partition into the bilayer to cause membrane disordering at a critical concentration (Seeman, 1972). This early concept of the action of alkanols derived from the studies of Overton (1901) and Meyer (1937). The potency of alkanols in producing anesthesia was reported to be linearly correlated with the log octanol-water partition coefficient (Seeman, 1972; Pringle, Brown & Miller, 1981; Requena et al., 1985; Elliott & Haydon, 1989; Abraham, Lieb & Franks, 1991). Lyon et al. (1981) suggested that alkanols act to disorder the bilayer to produce anesthesia.

Later work by Requena et al. (1985) showed that the anesthetic potency of a homologous series of primary alkanols to produce action potential (*AP*) block was correlated with the alkanol chain length. Requena et al. (1985) suggested that their data fit an alternative volume expansion hypothesis of anesthesia advanced by Mullins (1954) which suggested that adsorption of substances into the bilayer caused the molecules to exert their effect. Once a critical volume change occurred, anesthesia is produced.

Franks and Lieb (1984, 1986, 1994) and a number of other investigators (Ellena, Blazing & McNamee, 1983; Heidman, Oswald & Changeux, 1983) have suggested that anesthesia is produced by direct binding of anesthetics to appropriately sized pockets on ion channel proteins (especially ligand-gated channels). To assay for anesthetic binding and action, they used the firefly luciferase enzyme activity as a protein model system. Reduction in enzyme activity was used as a criterion of binding and anesthetic action. However, others (Requena, Moran & Malave, 1988; Alifimoff, Firestone & Miller, 1989) have criticized the appropriateness of the use of the firefly luciferase system as a model for the action of anesthetics.

* *Present address:* Department of Medicine, Division of Cardiology, The Johns Hopkins University School of Medicine, 720 North Rutland Ave., Ross 844, Baltimore, MD 21205, USA

*Correspondence to:* R. Hahin

In this study, a homologous series of *n*-alkanols was used to characterize the action of these molecules in blocking *AP*s in frog sciatic nerves. Since an aromatic ring is common to local anesthetics, a sequence of phenyl-substituted *n*-alkanols (Φ-alkanols) was also studied and compared with the series of *n*-alkanols to contrast their potencies and yield insight into the role the phenyl group plays in causing *AP* block. The results of this study showed that phenyl substitution significantly increased the potency of *n*-alkanols. The $ED_{50}$ for both groups of alkanols can be predicted as a function of the physical-chemical properties of the molecules. $ED_{50}$ can not simply be predicted by the size or the log $K_{OW}$.

## Materials and Methods

The single sucrose-gap method was used to record compound action potentials (*AP*s) from desheathed whole sciatic nerves from a frog (*Rana pipiens*). A more complete description of the method is found in Larsen, Gasser and Hahin (1996). A brief description of the method follows: a whole nerve was placed in a recording chamber with three separate compartments or pools (intracellular, extracellular, and stimulating) that contained solutions (*see* below). The sciatic nerve spanned all three compartments so that both ends were made to lie within the intracellular and stimulating pools. The intracellular compartment contained buffered 112 mM KCl solution, while the extracellular compartment contained Ringer's solution or Ringer's solution plus a test solute. The stimulating compartment contained Ringer's solution and was electrically isolated from the other two compartments via a Vaseline gap. The flow of sucrose was maintained at a constant rate of 6–8 ml/min so as to create an extracellular resistance of 5 MΩ/cm between the extracellular and intracellular compartments. A suction electrode was used to stimulate the nerve.

To insure the constancy of concentration of volatile solutes, the extracellular compartment was connected with a perfusion system. A volume flow rate of 0.3–0.5 ml/min was used and was sufficient to cause one volume of the extracellular pool to be replaced every minute. To reduce the rundown the intracellular KCl solution and stimulating pool Ringer's solutions were periodically replaced every 20–25 min.

Nerve *AP*s were differentially recorded between the intracellular and extracellular compartments. Stimuli were delivered to the nerve via a Model SD9 Stimulator (Grass Instrument, Quincy, MA). *AP*s were recorded on photographs (Polaroid CR10; Cambridge, MA) from repetitively applied traces on a VC 6524 Digital Storage Oscilloscope (Hitachi Denshi, Japan). All experiments were conducted at room temperature (20–22°C).

### Animals

Grass frogs (*Rana pipiens*) were purchased from Charles Sullivan, Nashville, TN.

### Solutions

Ringer's solution contained (in mM): 112 NaCl, 2 KCl, 2 $CaCl_2$, and 10 HEPES. The pH was adjusted to 7.4 with NaOH. The intracellular KCl solution contained in mM: 112 KCl and 20 HEPES. The pH was adjusted to 7.4 with KOH.

All test solutions were prepared using a volume per volume dilution of the test solute in Ringer's solution. The solutes used were: methanol, ethanol, *n*-propanol, *n*-butanol, *n*-heptanol, *n*-hexanol, benzyl alcohol, phenethyl alcohol, 3-phenyl-1-propanol, and phenol. The pH of all solutions was adjusted to 7.4. The osmolarity of each solute concentration was measured using an osmometer (Osmette, Precision Osmometer, Precisions Systems, Newton, MA). *n*-Propanol, benzyl alcohol, phenethyl alcohol, 3-phenyl-1-propanol were purchased from Aldrich Chemical, Milwaukee, WI, while methanol, ethanol *n*-butanol, *n*-heptanol, *n*-hexanol, and phenol were purchased from Sigma Chemical, St. Louis, MO.

### *AP* Data Analysis

The degree of *AP* block was defined to be the *AP* height in the solute divided by the pre-application control *AP* height obtained in Ringer's solution. *AP* heights were expressed as a fraction (relative *AP* heights) of control values. Error bars represent the mean ± SEM. If the symbols are larger than and obscure the error bars, the error bars were not shown in the figures. A 50% effective dose for *AP* block ($ED_{50}$) was defined to be the concentration of solute in Ringer's solution that produced a 50% reduction of the height of the control *AP*. $ED_{50}$s were obtained from each dose-response relation. The potency of each test solute was defined as a reciprocal of its $ED_{50}$ ($1/ED_{50}$). The relative potency (RP) of each solute was normalized so that methanol has a RP of 1. Statistical significance of difference in means was established at $P < 0.05$ using an unpaired *t*-test.

## Results

### Action Potential Stability in Ringer's Solution

In a series of experiments, *AP*s were recorded in Ringer's solution without the addition of any test solutes to determine the characteristic rate of *AP* rundown. Figure 1 shows *AP* stability in Ringer's solution observed in eight nerve preparations for 4–6½ hr. The initial maximum *AP* heights were normalized to best compare the rates of diminution of the *AP* height. Two distinctive patterns of *AP* rundown were observed. The first pattern shown by open symbols exhibited a fairly linear decline in height over 4–6½ hr. The other pattern, shown by filled symbols, showed a semiexponential decay that was much more rapid than the more stable linear pattern. Linear regression of the first group of *AP*s ($n = 5$) showed that progressive diminution of the *AP* in time was 3% per hr. *AP*s exhibiting the second more rapid decay were eliminated from the study. Therefore before applying test solutes, *AP*s were observed for 45–60 min to insure an acceptable *AP* decay.

The value of *AP* rundown for the five nerve preparations exhibiting a linear pattern of rundown shown in Fig. 1 was not significantly different from the rate of *AP* rundown recorded in the presence of the test solutes ($n = 36$). *AP* rundown determined in this study was similar to the rate of *AP* decay of 3% per hr for frog sciatic nerves reported previously by Bainton and Strichartz (1994). Acceptable *AP* rundown was less than 5% per hr.

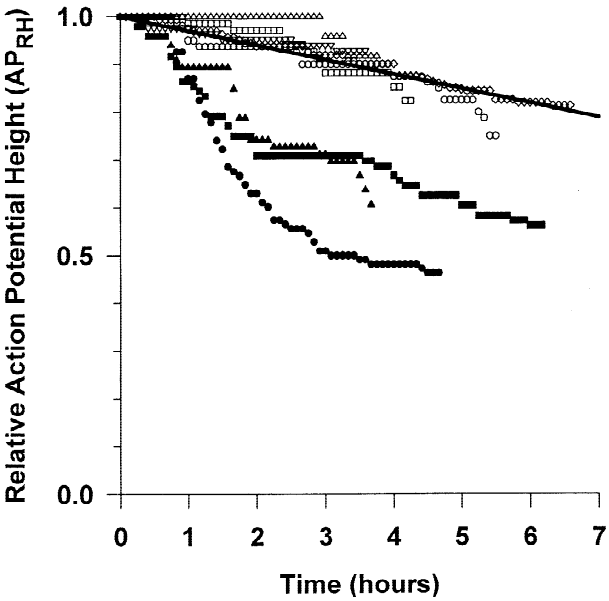


**Fig. 1.** *AP* rundown in Ringer's solution. Two different types of *AP* rundown are shown; open symbols represent a slow fairly linear *AP* decline and filled symbols represent a rapid semiexponential decay. Each plotted point represents the relative *AP* height recorded every 5 min after the *AP* reached its initial maximum height. The slow declining *AP* rundown was fit (solid line) using a linear least squares equation:

$$AP_{RH} = -0.03\ t + 1,\ (n = 5,\ r^2 = 0.85) \quad (1)$$

where $AP_{RH}$ is the *AP* relative height and $t$ is the time expressed in hours.

## Protocol to Obtain Dose-Response Relations for *AP* Block

To obtain dose-response relations for the solutes used, a sequence of at least five different concentrations of the solute in Ringer's solution with at least three replicates was applied to the extracellular pool bathing the nerve. Test solutes were applied to the nerves only after a nerve exhibited a stable *AP* amplitude for at least 45 min. For each reversibly acting solute, one dose was applied, followed by solute removal and recovery in Ringer's solution, before successive doses were applied to the nerve. Applications of low and high doses were randomized.

Figure 2 shows an example of a typical experiment. In this experiment, butanol was applied to a nerve at two different doses. The arrows indicate a change of solution. R indicates Ringer's solution and the numbers following the Rs indicate the number of successive Ringer's solution washes applied to the nerve. The additions of butanol at two different doses, 25 and 40 mM, are also indicated by the arrows.

Each *AP* was displaced to the right by approximately ½ of a division on the oscilloscope screen to indicate the passage of time following solution replacement. *AP*s were recorded every 5 min and thus each rightward displacement represents 5 min of elapsed time. Thus the kinetics of the onset and offset of block is shown by the envelope of *AP* peak heights after the addition or removal of a test solute. In this experiment, 40 mM butanol caused a greater degree of block than 25 mM butanol. The average recovery in all experiments was 97 ± 0.3% ($n = 292$).

## Dose-Response Relations for *AP* Block by *n*-Alkanols and Φ-Alkanols

Figure 3 represents dose-response relations plotted semilogarithmically for a series of seven *n*-alkanols in increasing chain length from methanol to heptanol. Each of the dose-response relations was fit by the logistics equation:

$$AP_{RH} = \frac{1}{1 + \left(\frac{c}{\mathrm{ED}_{50}}\right)^b} \quad (2)$$

where $AP_{RH}$ is the *AP* relative height, $c$ is the solute concentration in Ringer's solution, $ED_{50}$ is the half-blocking dose, and $b$ is the slope parameter. Best fit parameters for each logistics equation were obtained using a Marquardt-Levenberg nonlinear least square curve fitting algorithm. Figure 3 shows that increases in chain length cause a fairly uniform reduction in the $ED_{50}$ which can be observed as a leftward shift of each dose-response relation. These leftward shifts represent increases in potency caused by adding a methylene group to the carbon backbone of the molecule.

The rightmost dose-response relation (open circles) which represents methanol can be shifted leftward and superposes well onto every other dose-response relation; this shows that the slope for each relation is not significantly changed with an increase in chain length. Each leftward shift caused by the addition of a methylene group on average represents a 3.2-fold increase in relative potency. These results are similar to those seen by Requena et al. (1985).

The open symbols in Fig. 4 represent the identical dose-response relations shown in Fig. 3 for methanol, ethanol, and *n*-propanol while the filled symbols represent dose-response relations for their phenyl-substituted homologues. The curves represent best fit logistics equation descriptions of the relations. Also shown in Fig. 4, indicated by an interrupted logistics fit (open diamonds), is the dose-response relation for phenol. The dose-response relations for the phenyl-substituted homologues of *n*-alkanols shown in Fig. 4 appear as leftward shifted versions of the dose-response relations of their unsubstituted counterparts.

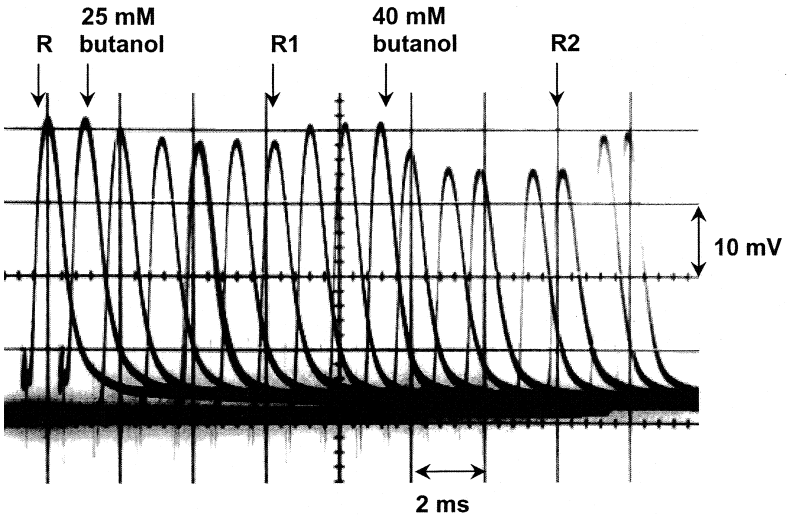


**Fig. 2.** Example of a typical solute application to a nerve. The kinetics of the onset and offset of *AP* block observed during applications of two concentrations of *n*-butanol (25 and 40 mM) are shown. The first two *AP*s (denoted R) were recorded in Ringer's solution prior to the addition of *n*-butanol and served as the control *AP* height. Thereafter, successive Ringer's solution washouts are denoted by an *R* followed by a number. *AP*s were recorded every 5 min and rightward shifted approximately ½ division to indicate the passage of time.

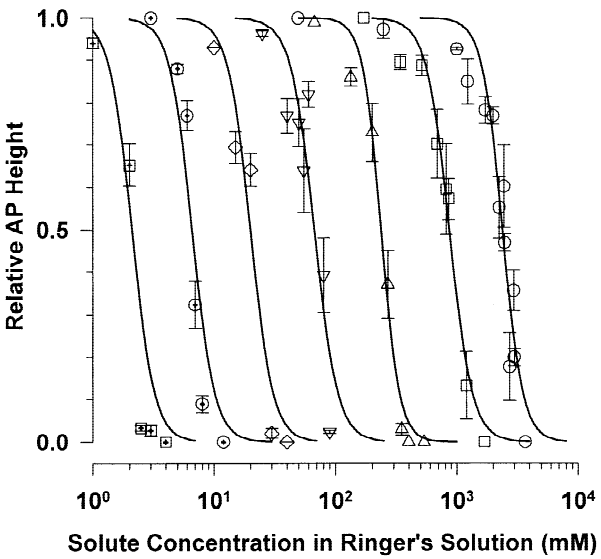


**Fig. 3.** Dose-response relations for *AP* block by *n*-alkanols. Dose-response relations for a series of *n*-alkanols are shown in the order of increasing chain length from methanol (rightmost, open circles) to *n*-heptanol (leftmost, cross-centered squares). The other symbols represent: ethanol (open squares), *n*-propanol (open upright triangles), *n*-butanol (open triangles), *n*-pentanol (open diamonds), and *n*-hexanol (cross-centered circles). Each plotted point represents the mean relative height of the *AP* ± SEM at a particular concentration of a test solute in Ringer's solution. Solid traces represent nonlinear least squares fits to each dose-response curve using the logistic equation.

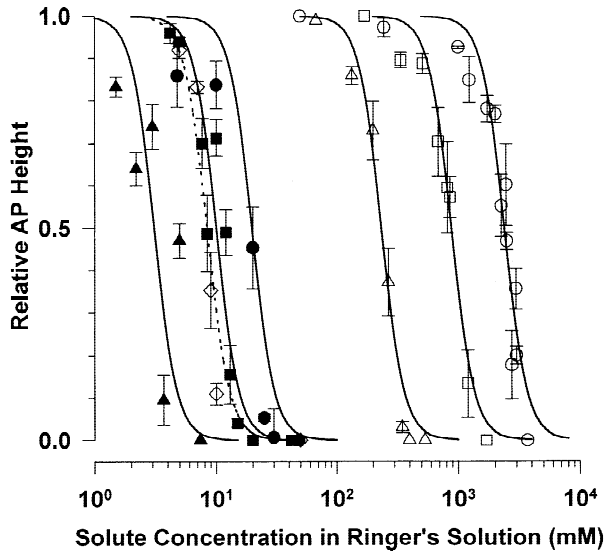


**Fig. 4.** Dose-response relations for *AP* block by *n*-alkanols and their phenyl substituted counterparts and phenol. Three successively larger *n*-alkanols shown on the right-hand side, methanol (open circles), ethanol (open squares), and propanol (open triangles) and their phenyl-substituted *n*-alkanol counterparts, benzyl alcohol (filled circles), phenethyl alcohol (filled squares), and 3-phenyl-1-propanol (filled triangles) are shown. For comparison purposes the dose-response relation for phenol is indicated by open diamonds. Each plotted point represents the *AP* height relative mean ± SEM at a particular concentration of a test solute in Ringer's solution. Traces represent nonlinear least squares fits to each dose-response curve using the logistic equation.

Similar to *n*-alkanols, the addition of a methylene group to a Φ-alkanol increases its potency and produces a shift in its dose-response relation. When compared with its unsubstituted *n*-alkanol counterpart, each phenyl-substituted dose-response relation is leftward shifted by a minimum of 1.9 log units by the addition of a phenyl group to the *n*-alkanol. The potency increase caused by the addition of a phenyl group, indicated by the shift in the dose-response relations, decreased when the chain length increased; as the chain length increased from one to three carbons the potency increased by 122-, 89-, and 77-fold, respectively. This suggests that the potency increases attributed to the increase in size due to the addition of a phenyl group are less effective as the chain length increases.

**Table 1.** $ED_{50}$s and potencies for AP block

| Solute | $ED_{50}$ (mM) | RP | ∂ potency/∂ $CH_2$ | *b* | Log $K_{OW}$ |
|---|---|---|---|---|---|
| *n*-Alkanols | | | | | |
| Methanol | 2392 ± 54 | 1 | | 4.9 ± 0.7 | −0.77 |
| Ethanol | 881 ± 30 | 2.7 | 2.7 | 4.4 ± 0.8 | −0.31 |
| *n*-Propanol | 235 ± 8 | 10 | 3.7 | 5.2 ± 0.8 | 0.25 |
| *n*-Butanol | 69 ± 3 | 35 | 3.4 | 4.6 ± 0.9 | 0.88 |
| *n*-Pentanol | 20 ± 1 | 118 | 3.5 | 4.3 ± 0.7 | 1.56 |
| *n*-Hexanol | 6.6 ± 0.6 | 343 | 3 | 4 ± 1.9 | 2.03 |
| *n*-Heptanol | 2.2 ± 0.1 | 1046 | 3 | 4 ± 0.9 | 2.72 |
| Mean ± SEM | | | 3.2 ± 0.15 | 4.48 ± 0.17 | |
| Phenol and Φ-alkanols | | | | | |
| Phenol | 8.1 ± 0.3 | 295 | | 5 ± 1.1 | 1.46 |
| Benzyl alcohol | 20 ± 0.5 | 122 | | 4 ± 1.2 | 1.10 |
| Phenethyl alcohol | 10 ± 0.6 | 240 | 2 | 3.9 ± 1 | 1.51 |
| 3-Phenyl-1-propanol | 3.1 ± 0.2 | 771 | 3.2 | 3.4 ± 1 | 2.05 |
| Mean ± SEM | | | | 4.08 ± 0.34 | |

$ED_{50}$–50% AP blocking concentration.
RP–solute potency relative to methanol.
∂ potency/∂ $CH_2$–increase in potency with the addition of a $CH_2$ group.
*b*–slope parameter used to fit equation: relative $AP = 1/1 + (c/ED_{50})^b$, where *c* is a solute concentration.
$K_{OW}$–octanol-water partition coefficient.

## $ED_{50}$s for *AP* Block

Table 1 tabulates the experimentally obtained values of $ED_{50}$ along with log $K_{OW}$s obtained from Kamlet et al. (1988) and Tayar et al. (1991) for all test solutes used. Also shown in Table 1 are the relative potencies (RP), the change in potency caused by the addition of a methylene group to the carbon backbone of the molecule (∂ potency/∂ $CH_2$), and the slope parameter (*b*) used in Eq. 2 to describe $AP_{RH}$. The RPs of solutes were assigned values relative to methanol by equating the RP of methanol to 1. As expected, $ED_{50}$s declined by increasing the chain length of both groups of alkanols. For *n*-alkanols, the $ED_{50}$s decreased (and potencies increased) on average by a factor of 3.2 ± 0.15 for each methylene group added to the molecule. Successive increases in chain length ultimately caused *n*-heptanol to be 1,000 times more potent than methanol.

The slope parameter (*b*) did not significantly change in amplitude as the size of the alkanol increased. The means for the slope parameters for *n*-alkanols and Φ-alkanols were not significantly different; the mean slope parameter for all solutes was 4.34 ± 0.166. As expected from previous works (Seeman, 1972; Janoff et al., 1981), the RP of an alkanol increases as the log $K_{OW}$ increases, suggesting that lipid solubility is an important determinant of potency.

## Alkanol Size, Log $K_{OW}$, and $ED_{50}$

Table 2 compiles $ED_{50}$s, $K_{OW}$s, and the physico-chemical properties for each of the solutes used. To characterize the relationship between size and $ED_{50}$, $ED_{50}$ was plotted *vs.* the number of methylene groups in the backbone of the molecule (Fig. 5). The open and filled symbols show the relationships between $ED_{50}$ and the number of methylene groups for *n*-alkanols and Φ-alkanols, respectively. The open diamond represents phenol. Figure 5 shows that the logarithm of the $ED_{50}$ decreases linearly with an increase in the chain length of the molecule. The slopes of the two log $ED_{50}$ *vs.* $CH_2$ group number relations were not significantly different. The linear relation observed for Φ-alkanols can be interpreted to represent a downward shifted version of the relation for *n*-alkanols. With this interpretation, the addition of a phenyl group to a parent molecule simply increased its potency without altering the relationship between the $ED_{50}$ and the number of $CH_2$s in the backbone of the molecule. The $ED_{50}$ value for phenol, which possesses an aromatic ring common to Φ-alkanols but lacks the carbon backbone, was plotted for comparison purposes. Phenol, despite its smaller size than benzyl alcohol, was more potent. The $ED_{50}$ value of phenol was smaller than the zero $CH_2$ extrapolated value obtained from extending the linear relation for Φ-alkanols to zero methylene groups.

To determine whether the solute lipid solubility can solely determine *AP* blocking potency, $ED_{50}$s were plotted on a logarithmic scale as a function of their log $K_{OW}$. Figure 6 shows plots of the log $ED_{50}$ *vs.* log $K_{OW}$ relations for both groups of alkanols; the open and closed symbols represent the relations for *n*-alkanols and Φ-alkanols, respectively. The open diamond represents phenol. The slopes of the two log $ED_{50}$ *vs.* log $K_{OW}$ relations were not significantly different. No single relation

**Table 2.** Experimentally obtained $ED_{50}$s and physico-chemical properties of solutes

| Solute | $ED_{50}$ (mM) | Physico-chemical properties | | | | |
|---|---|---|---|---|---|---|
| | | $V_l/100$ | $P$ | β | α | log $K_{OW}$ |
| *n*-Alkanols | | | | | | |
| Methanol | 2392 ± 54 | 0.205 | 0.40 | 0.42 | 0.35 | −0.77 |
| Ethanol | 881 ± 30 | 0.305 | 0.40 | 0.45 | 0.33 | −0.31 |
| *n*-Propanol | 235 ± 8 | 0.405 | 0.40 | 0.45 | 0.33 | 0.25 |
| *n*-Butanol | 69 ± 3 | 0.499 | 0.40 | 0.45 | 0.33 | 0.88 |
| *n*-Pentanol | 20 ± 1 | 0.593 | 0.40 | 0.45 | 0.33 | 1.56 |
| *n*-Hexanol | 6.6 ± 0.6 | 0.690 | 0.40 | 0.45 | 0.33 | 2.03 |
| *n*-Heptanol | 2.2 ± 0.1 | 0.788 | 0.40 | 0.45 | 0.33 | 2.72 |
| Phenol and Φ-alkanols | | | | | | |
| Phenol | 8.1 ± 0.3 | 0.536 | 0.72 | 0.33 | 0.61 | 1.46 |
| Benzyl alcohol | 20 ± 0.5 | 0.634 | 0.99 | 0.52 | 0.39 | 1.10 |
| Phenethyl alcohol | 10 ± 0.6 | 0.732 | 0.97 | 0.55 | 0.33 | 1.51 |
| 3-Phenyl-1-propanol | 3.1 ± 0.2 | 0.830 | 0.95 | 0.55 | 0.33 | 2.05 |

$ED_{50}$–solute concentration producing 50% block.
$V_l/100$–intrinsic molar volume/100 (ml/M × $10^{-2}$).
$P$–polarity (high frequency polarizability).
β–hydrogen bond acceptor basicity.
α–hydrogen bond donor acidity.
$K_{OW}$–octanol-water partition coefficient.

between the log $ED_{50}$ and the log $K_{OW}$ can predict the behavior of both groups of molecules. This suggests that log $K_{OW}$ does not solely determine the $ED_{50}$.

## Discussion

### Comparison of Results

The earliest studies of the anesthetic action of *n*-alkanols were designed to characterize the alkanol-induced blocking effect on either whole animal behavior or tissue function. For example, *n*-alkanols effectively blocked righting reflexes in tadpoles (Pringle et al., 1981; Alifimoff, Firestone & Miller, 1989) and mice (Lyon et al., 1981) and the escape response in freshwater shrimp (Elliott, Haydon & McElwee, 1986). Similarly, the function of various tissues obtained from different organs was reduced in the presence of *n*-alkanols (Rang, 1960; Lyon et al., 1981). The anesthetic action of *n*-alkanols on many species was studied including paramecia and guinea pigs (Rang, 1960), fireflies (Franks & Lieb, 1984; Moss et al., 1991), tadpoles (Pringle et al., 1981; Alifimoff et al., 1989), mice (Lyon et al., 1981), and the freshwater shrimp (Elliott et al., 1986). Consistent with the results reported in this study, the overall results of these previous studies suggested that the anesthetic action of *n*-alkanols increased with an increase in the size of the molecule and correlated well with their octanol-water partition coefficients.

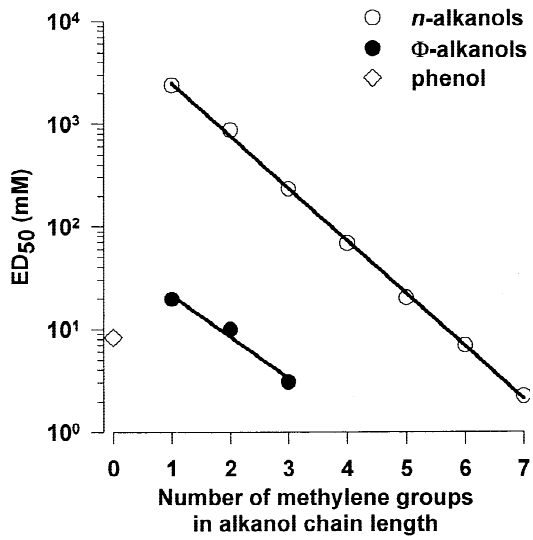


**Fig. 5.** $ED_{50}$ *vs.* alkanol chain length relations. The log $ED_{50}$s for *n*-alkanols (open circles) and Φ-alkanols (filled circles) were plotted *vs.* the number of methylene groups in the carbon backbone of each molecule. The open diamond represents the $ED_{50}$ value for phenol. The lines represent linear least squares fits for the two sets of data and represent the following equations:

$ED_{50} = 8121/(3.25^N)$ ($r^2 = 0.999$, $n = 180$) *n*-alkanols,

$ED_{50} = 54/(2.52)^N$) ($r^2 = 0.977$, $n = 97$) Φ-alkanols,

where $N$ is the number of methylene groups and $N < 12$, $r$ is the correlation coefficient, and $n$ is the number of observations.

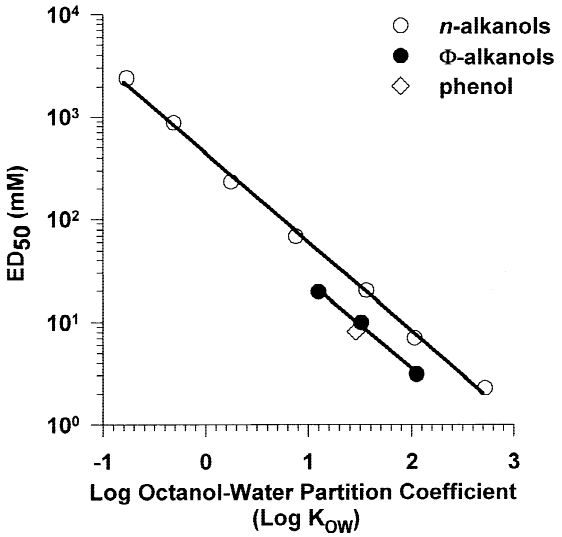


**Fig. 6.** Log $ED_{50}$s *vs.* log $K_{OW}$ relations for *n*-alkanols and Φ-alkanols. The $ED_{50}$ for *n*-alkanols (open circles) and Φ-alkanols (filled circles) were plotted *vs.* the log $K_{OW}$. The open diamond represents the $ED_{50}$ value for phenol. The lines represent linear least squares fits for the two sets of data.

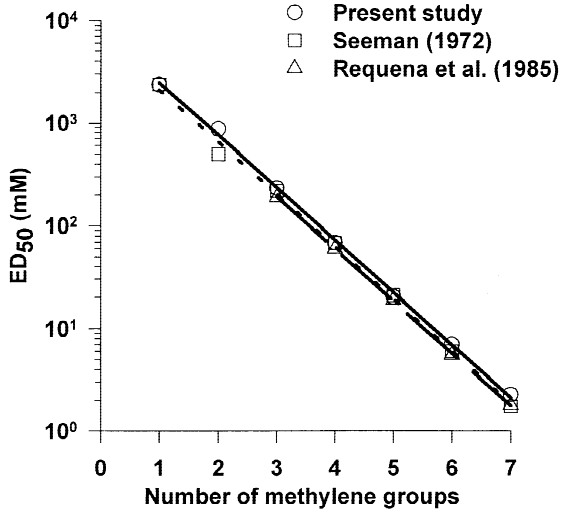


**Fig. 7.** $ED_{50}$ *vs.* chain length relations for *n*-alkanols from three separate studies. The $ED_{50}$ values for *n*-alkanols obtained in the present study (open circles), by Seeman, 1972 (open squares), and by Requena et al., 1985 (open triangles) were plotted *vs.* the number of methylene groups in an *n*-alkanol. Each data set was individually fit with a linear least square relation. Each of the three linear least square relations was not significantly different from each other when pairwise comparisons were made with a *t*-test.

Sequences of *n*-alkanols have been previously shown to block *AP*s in frog and toad sciatic nerves (Seeman, 1972; Requena et al., 1985), and squid giant axons (Armstrong & Binstock, 1964; Seeman, 1972; Haydon & Urban, 1983). The most comprehensive compilations of data describing alkanol-induced *AP* block were works by Seeman (1972) and Requena et al. (1985). Figure 7 compares previously published results of *AP* block with results obtained in this study. In common, all three *AP* studies have examined the action of *n*-alkanols from *n*-propanol to *n*-heptanol. Seeman (1972) also obtained $ED_{50}$ values for methanol, ethanol, phenol, and benzyl alcohol; this study extends the $ED_{50}$ data to include phenethyl alcohol and 3-phenyl-1-propanol. In common with previous results reported on alkanol action on animal behavior or tissue function, Figure 7 shows that the $ED_{50}$ decreases with an increase in the size of the molecule. From each study, each data set was individually fit with a linear relation between $ED_{50}$ and the number of methylene groups present in the *n*-alkanol. The relations were not significantly different when pairwise comparisons were made. Thus the $ED_{50}$ *vs.* size relations obtained for *AP* block for *n*-alkanols in this study were consistent with previously reported results using *n*-alkanols.

## Predictions of $ED_{50}$

Using the data from Fig. 6, two separate equations were derived to describe $ED_{50}$ *vs.* the corresponding log $K_{OW}$ for *n*-alkanols and Φ-alkanols. Using the parameters from the best fit equations for both groups of alkanols the following equations were obtained for *n*-alkanols and Φ-alkanols, respectively:

$$ED_{50} = 449/(K_{ow}{}^{0.86}) \; (r^2 = 0.998, \, n = 180) \; n\text{=alkanols} \tag{3}$$

$$ED_{50} = 177/(K_{ow}{}^{0.86}) \; (r^2 = 0.995, \, n = 97) \; \Phi\text{=alkanols} \tag{4}$$

where $r$ is the correlation coefficient and $n$ is the number of observations.

Using the assumptions of the theory of linear salvation energy relations, LSER (Taft et al., 1985), an equation for the log $ED_{50}$ can be mathematically predicted as a function of size, polarity, and hydrogen bond acceptor basicity and donor acidity. Using multiple linear regression analysis the following equation results:

$$\mathrm{ED}_{50} = 10^{(-5.36\, V_I + 0.88\, \mathrm{P} - 1.06\, \beta - 4.92\, \alpha + 6.29)}, \quad (r^2 = 0.999) \tag{5}$$

where $V_I$ is the solute intrinsic molar volume, $P$ is the polarity, β and α are the hydrogen bond acceptor basicity and donor acidity, respectively, and $r$ is the correlation coefficient. This equation predicts the $ED_{50}$s for both *n*-alkanols and Φ-alkanols. The predictions are excellent for chain lengths up to dodecanol ($C = 12$). In other words, the equation is valid for values of $V_I$ that range from 0.205 through 1.273. The $ED_{50}$ cannot simply be

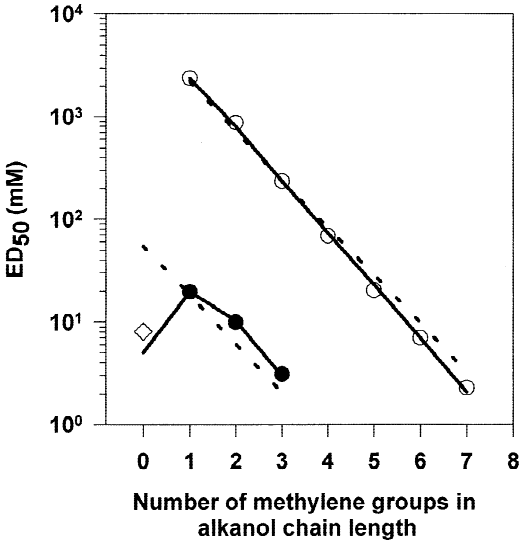


**Fig. 8.** Experimental and predicted $ED_{50}$ values. A comparison of two alternative predictions of $ED_{50}$ for alkanols and phenol. Shown above are experimentally obtained $ED_{50}$ values for *n*-alkanols (open circles), Φ-alkanols (filled circles), and phenol (open diamond). Predictions obtained from a linear combination of $V_l$, $P$, β, and α (Eq. 5) are shown as solid traces. Alternative predictions obtained by using $V_l$ as the only independent variable are shown as dotted traces:

$$ED_{50} = 10^{(-4.79\ Vl + 4.23)},\ (r^2 = 0.921) \quad (6)$$

where $V_l$ is the intrinsic molar volume and $r$ is the correlation coefficient.

predicted by log $K_{OW}$ or the size alone: However, Eq. 5 is only valid for primary alkanols.

Figure 8 shows $ED_{50}$ values for *n*-alkanols (open circles), Φ-alkanols (filled circles), and phenol (open diamond) and predictions from Eq. 5 (solid traces) and predictions based on the size alone (dotted traces). The size variable (the intrinsic molar volume) is the most important predictor variable of the four variables in Eq. 5. However, if only size was used to predict the $ED_{50}$, the discrepancies between the predicted and experimentally obtained values continuously diverge as the chain length increased above three carbons for *n*-alkanols and it failed to predict $ED_{50}$s for the two larger Φ-alkanols.

If $V_l$ is the sole predictor of the $ED_{50}$, the $ED_{50}$ for phenol was predicted to be the value expected for a "theoretical zero carbon chain length Φ-alkanol." This value is exactly the zero value extrapolated from the linear relation between log $ED_{50}$ and the number of methylene groups for Φ-alkanols. Thus a prediction based on size alone gives poor values for Φ-alkanols and provides a completely erroneous value for phenol. However, predictions based on Eq. 5 fit all the experimentally observed $ED_{50}$ values for *n*- and Φ-alkanols very well. The observed $ED_{50}$ for phenol is also fairly well predicted showing that properties of the molecule other than the size cause changes in *AP* block. Two other variables used in the prediction (α and β) play key roles in binding interactions between molecules such as alkanols and membrane proteins.

Equation 5 shows how phenyl substitution causes increases in alkanol potency: The addition of a phenyl group causes an increase in the hydrogen bond acceptor basicity of the molecule which allows the molecule to more easily make hydrogen bonds with other donor molecules. If alkanols interact with Na channels to exert their *AP* blocking effect (Kondratiev & Hahin, 2001), increases in β would contribute to increased binding of the Φ-alkanol to hydrogen bond donor sites of the Na channel. Thus these results are consistent with the idea that alkanols bind to and interact with Na channels to cause *AP* block.

## References

Abraham, M.H., Lieb, W.R., Franks, N.P. 1991. Role of hydrogen bonding in general anesthesia. *J. Pharm. Sci.* **80:**719–724

Alifimoff, J.K., Firestone, L.L., Miller, K.W. 1989. Anaesthetic potencies of primary alkanols: implications for the molecular dimensions of the anesthetic site. *Brit. J. Pharmacol.* **96:**9–16

Armstrong, C.M., Binstock, L. 1964. The effects of several alcohols on the properties of the squid giant axon. *J. Gen. Physiol.* **48:**265–277

Bainton, C.R., Strichartz, G.R. 1994. Concentration dependence of lidocaine-induced irreversible conduction loss in frog nerve. *Anesthesiology* **81:**657–667

Ellena, J.F., Blazing, M.A., McNamee, M.G. 1983. Lipid-protein interactions in reconstituted membranes containing acetylcholine receptor. *Biochemistry* **22:**5523–5535

Elliott, J.R., Haydon, D.A. 1989. The action of neutral anaesthetics on ion conductances of nerve membranes. *Biochemica et Biophysica Acta,* **988:**257–286

Elliott, J.R., Haydon, D.A., McElwee, A.A. 1986. A comparison of the potencies of *n*-alkanols methyl carboxylic esters as general anaesthetics in *Gammarus* and as local anaesthetics in isolated axons of *Loligo. Physiol. Soc.* 21 *P*

Franks, N.P., Lieb, W.R. 1984. Do general anesthetics act by competitive binding to specific receptors? *Nature* **310:**399–401

Franks, N.P., Lieb, W.R. 1986. Partitioning of long-chain alcohols into lipid bilayers: Implications for mechanisms of general anesthesia. *Proc. Nat. Acad. Sci. USA* **83:**5116–5120

Franks, N.P., Lieb, W.R. 1994. Molecular and cellular mechanisms of general anesthesia. *Nature* **367:**607–614

Haydon, D.A., Urban, B.W. 1983. The action of alcohols and other non-ionic surface active substances on the sodium current of the squid giant axon. *J. Physiol.* **341:**411–427

Heidman, T., Oswald, R.E., Changeux, J.-P. 1983. Multiple sites of action for noncompetitive blockers on acetylcholine receptor rich membrane fragments from *Torpedo marmorata. Biochemistry* **22:**3112–3127

Janoff, A.S., Pringle, M.J., Miller, K.W. 1981. Correlation of general anesthetic potency with solubility in membranes. *Biochim. Biophys. Acta* **649:**125–128

Kamlet, M.J., Doherty, R.M., Abraham, M.H., Marcus, Y., Taft, R. 1988. Linear solvation energy relationships. 46. An improved equation for correlation and prediction of octanol/water partition coefficients of organic nonelectrolytes (including strong hydrogen bond donor solutes). *J. Phys. Chem.* **92:**5244–5255

Kondratiev, A. Hahin, R. 2001. $ED_{50}$ GNa block predictions for phenyl-substituted and unsubstituted *n*-alkanols. *J. Membrane Biol.* **180:**123–136

Larsen, J., Gasser, K., Hahin, R. 1996. An analysis of dimethylsulfoxide-induced action potential block: A comparative study of DMSO and other aliphatic water soluble solutes. *Toxicol. Appl. Pharmacol.* **140:**296–314

Lyon, C.R., McComb, J.A., Schreurs, J., Goldstein, D.B. 1981. A relationship between alcohol intoxication and the disordering of brain membranes by a series of short-chain alcohols. *J. Pharmacol. Exp. Ther.* **218:**669–675

Meyer, K.H. 1937. Contributions to the theory of narcosis. *Trans. Faraday Society* **33:**1062–1068

Moss, G.W.J., Franks, N.P., Lieb, W.R. 1991. Modulation of the general anesthetic sensitivity of a protein: A transition between two forms of firefly luciferase. *Proc. Natl. Acad. Sci. USA* **88:**134–138

Mullins, L.J. 1954. Some physical mechanisms of narcosis. *Chemical Review* **54:**289–323

Overton, E. 1901. Studien uber die narkose. *Jena. Verlag Gustaf Fischer*

Pringle, M.J., Brown, K.B., Miller, K.W. 1981. Can the lipid theory of anesthesia account for the cutoff in anesthetic potency in homologous series of alcohols? *Mol. Pharmacol.* **19:**49–55

Rang, H.P. 1960. Unspecific drug action. The effects of a homologous series of primary alcohols. *Brit. J. Pharmacol.* **15:**185–200

Requena, J., Haydon, D.A. 1985. Is there a "cut-off" in the adsorption of long chain amphipathic molecules into lipid membranes? *Biochemica et Biophysica Acta* **814:**191–194

Requena, J., Moran, O., Malave, P. 1988. A comparison of the effect of experimental anesthetics on nerve impulse blockade and on a proteinaceous site. *Biochem. Biophys. Res. Commun.* **54:**47–53

Requena, J., Velaz, M.E., Guerrero, J.R., Medina, J.D. 1985. Isomers of long-chain alkane derivatives and nervous impulse blockage. *J. Membrane Biol.* **84:**229–238

Seeman, P. 1972. The membrane actions of anesthetics and tranquilizers. *Pharmacol. Rev.* **24:**583–655

Taft, R.W., Abraham, M.H., Famini, G.R., Doherty, R.M., Abboud, J-L.M., Kamlet, M.J. 1985. Solubility properties of polymers and biological media 5: An analysis of physiochemical properties which influence octanol-water partition coefficients of aliphatic and aromatic solutes. *J. Pharm. Sci.* **74:**807–814

Tayar, N.E., Tsai, R.-S., Testa, B., Carrupt, P.-A., Leo, A. 1991. Partitioning of solvents in different solvent systems: the contribution of hydrogen-bonding capacity and polarity. *J. Pharm. Sci.* **80:**590–598